ANIMAL MODELS OF DIABETIC COMPLICATIONS CONSORTIUM
University of Michigan
(U01 DK60994)

UPDATE REPORT
(September 2001 –January 2004)

Eva L. Feldman, M.D., Ph.D.
Neuropathy Phenotyping Core

Eva L. Feldman, M.D., Ph.D.
University of Michigan
Department of Neurology
Ann Arbor, MI 48109-0676
Phone: (734) 763-7274 Fax: (734)763-7275
Email: efeldman@umich.edu

Table of Contents

A. Rationale and Relevance

Although several animal models of diabetic neuropathy exist, the pathological abnormalities in the rodent peripheral nerve do not duplicate those encountered in human neuropathy (1, 2). Many animal models of diabetes i.e. the STZ rat and mouse models and the BB Wistar and Zucker diabetic rat develop nerve conduction changes consistent with an axonal neuropathy, similar to those seen in the diabetic patient (1). In human neuropathy, these nerve conduction changes are associated with axonal degeneration (3-5). However, while nerve conduction slows in animal models, the changes of axonal degeneration may not be observed (1, 2). Another concern is the difficulty in correlating hyperglycemia with pathology. In the diabetic (insulin-dependent) diabetic BB/Wor rat, neuropathy is far more severe than in the BBZDR/Wor rat (a model of type II diabetes), despite similar levels of glycemic control (1, 2). Thus, even this diabetic rat may not closely model human neuropathy. The reasons for the resistance to full-blown complications are likely manifold, but may include absence of important genetic susceptibility genes and, more simply, the life-span of rodents is too limited to allow full development of complications. This latter reason may be paramount since the onset and evolution of diabetic complications are quite gradual in humans. One of the goals of the AMDCC is to develop animal models of diabetic neuropathy that more closely resemble the human condition. The Neuropathy Core was established at the onset of the AMDCC to determine if new mouse models of diabetic neuropathy had a phenotype that resembled the neuropathic condition in man. The Neuropathy Core was also mandated to assist in the development of these new mouse models of diabetic neuropathy.

B. Summary of Accomplishments

The Neuropathy Phenotyping Core has instituted the guidelines for assessing the presence of neuropathy in diabetic animals.

From its inception, the Core uses phenotyping criteria in animals that parallel the clinical criteria used in man. A mouse model of diabetic neuropathy requires the key features present in the human condition (6-9). These include:

1. *Evidence of clinical loss of sensory function*
2. *Electrophysiological evidence of nerve impairment*
3. *Anatomical evidence of nerve fiber loss*

In man, diabetic neuropathy is a progressive disorder, with signs and symptoms that parallel the loss of nerve fibers that occurs overtime with poor glycemic control (9, 10). Consequently, assessments of neuropathy in mice are not performed at one time point, but are characterized at multiple time points during a 6 month period of diabetes and correlated with glycemic control. Diabetic control is evaluated in 2 ways: tail blood glucose measured following a 6 hour fast and glycated hemoglobin levels. The initial degree of neuropathy is screened using the 3 methods discussed below. Detailed measures of neuropathy are employed when the initial screening instruments indicate a profound or unique phenotypic difference.

Phenotyping of Mice for the Presence of Diabetic Neuropathy

Evidence of clinical loss of sensory function

The progressive distal to proximal loss of nerve fiber function in animals with diabetes leads to decreased sensation in the animal's paws and tail. Quantitative assessment of sensory function reflects the loss of nerve function. The first component of mouse phenotyping for the presence of diabetic neuropathy is a quantitative assessment of paw and tail sensation. The time of withdrawal from a heat stimulus applied separately to the paw or to the tail is measured on a monthly basis.

Electrophysiological evidence of nerve impairment

Electrophysiology is considered the "gold standard" for evaluation of neuropathic deficits in man. Nerve conduction studies provide a quantitative measurement of sensory and motor nerve function. The second component of mouse phenotyping for the presence of diabetic neuropathy is assessment of motor and sensory nerve conductions.

Anatomical evidence of nerve fiber loss

Deficits in motor or sensory function may be caused by disruptions of axonal function or axonal loss. Analysis of myelinated fiber density, peripheral nerve structure and intraepidermal fiber density all lend insight into the function of the peripheral nervous system. The third component of mouse phenotyping is assessment of small myelinated and unmyelinated fibers using serial skin biopsies.

Advanced measures of neuropathy

When the initial screening of a mouse model indicates the presence of a profound or unique neuropathy, a more detailed analysis will be performed. These analyses include transmission electron microscopy (TEM), poly TdT mediated dUTP-biotin nick end labeling (TUNEL), immunohistochemistry (IHC) for cleaved caspase-3, and oxidative stress adducts and biochemical measures of oxidative stress adducts and enzyme activity.

The Neuropathy Phenotyping Core has been an integral part in developing new mouse models of diabetic neuropathy.

Rodent models of diabetes fail to develop changes that closely resemble human diabetic nephropathy or neuropathy. While the reasons for the resistance of rodents to full-blown complications are likely multiple, they may include an increased resistance to oxidative stress or the absence of important genetic susceptibility genes (11, 12). Our general strategic approach to this dilemma is to accelerate the injury of diabetes by predisposing critical cells within the peripheral nervous system, including sensory neurons and their supporting Schwann cells, to glucose-mediated oxidative injury by 1) increasing glucose uptake via increased expression of facilitative glucose transporters or 2) by reduction of enzymes that reduce oxidative stress.

This report of our accomplishments presents a chronological account of our approach and resulting data in developing and phenotyping new mouse models of diabetic neuropathy. The report is organized chronologically by years and, within each year, by model (see Table 1).

Table 1 **Mouse Strains**

Animal model	Background strain	Current Status	Phenotyping (begin-end)	Consortium Collaborators
db/db	C57BL/6J	breeding; phenotyping complete	9-03 breeding stock	
db/db	C57B.KLS	breeding; begin neuro phenotyping	2-04 to 3-05; breeding stock	
SOD2 +/- STZ	C57BL/6J	Phenotyping complete; no increase in neuropathy	3-02 to 8-03	
SOD2 +/- db/db	C57BL/6J	Phenotyping complete; no increase in neuropathy	3-03 to 9 -03	
nestin Cre//SOD2 loxP/loxP	C57BL/6J	breeding currently	3-04 to 2-05	
synapsin Cre//SOD2 loxP/loxP	C57BL/6J	breeding currently	4-04 to 4-05	
AR tg//SOD2+/- STZ	C57BL/6	phenotyping ongoing; increased neuropathy in diabetics with double mutation	1-04 to 12-04	
AR tg//SOD2+/- db/db	C57BL/6	breeding	6-04 to 5-05	
GCLC +/- STZ	C57BL/6J	on hold	6-03 to 5-04	
GCLC +/- db/db	C57BL/6J	phenotyping ongoing	7-03 to 6-04	
fyn -/-	C57BL/6J 129SvJ	phenotyping complete severe albuminuria in nondiabetics	6-03 to 8-03	
fyn -/- STZ	C57BL/6J 129SvJ	phenotyping completed: increased albuminuria in diabetics with mutation	6-03 to 8-03	
fyn -/-	129SvJ	rederivation completed; phenotyping ongoing. No albuminuria in nondiabetics	9-03 to 8-04	
fyn -/- and +/- STZ	129SvJ	phenotyping ongoing	9-03 to 9-04	
synapsin cre	C57BL/6J	crossed with Rosa26	breeding stock	
nestin cre	C57BL/6J	crossed with Rosa26	breeding stock	

Year 1

SOD2 +/- STZ diabetic mice. Mitochondrial superoxide dismutase (SOD2) detoxifies highly reactive superoxide (O_2^-) by catalysis to hydrogen peroxide, which in turn is reduced in mitochondria by glutathione. The SOD2 -/- mice have a severe reduction in succinate dehydrogenase (complex II) and aconitase (a TCA cycle enzyme) activities suggesting that SOD2 maintains the integrity of mitochondrial enzymes susceptible to direct inactivation by superoxide. These abnormalities lead to cardiomyopathy and neurodegeneration with neonatal lethality. The SOD2 +/- animals have reduced enzyme activity in mitochondria from many tissues, show increased mitochondrial oxidative stress, and have increased mitochondrial swelling due to induction of the permeability transition pore but have no major pathophysiologic abnormalities and no neurodegeneration or nephropathy has been reported. Since the SOD2 -/- mice could not be used for long-term experiments, we reasoned that SOD2 +/- mice, which are viable, would still be susceptible to oxidative stress and diabetic complications. Two experiments were completed with essentially identical results. In the first experiment, there were 6 mice per group. In the second experiment, there were 10 mice per group. Data will be presented from the second larger experiment. Animals were made diabetic per the AMDCC protocol and monthly fasting tail blood glucoses confirmed diabetes. The 4 experimental groups were (C=control, D=streptozotocin diabetes): SOD2+/-D, SOD2+/+D, SOD2+/-C, SOD2+/+C. Diabetic animals remained hyperglycemic throughout the 6 month time period as evidenced by glycated hemoglobin measurements at 24 weeks: SOD2+/-D, 9.63 $\pm$ 0.7; SOD2+/+D, 11.2 $\pm$ 0.3; SOD2+/-C, 4.7 $\pm$ 0.1; SOD2+/+C, 4.9 $\pm$ 0.3.

To assess for the presence of diabetic neuropathy, tail flick analyses and nerve conductions studies were completed at 8, 12, 16, 20 and 24 weeks on the 4 groups. The tail flick analysis constitutes a validated and quantitative assessment of sensory function. The "tail flick" consists of measurements of the time needed for an animal to withdraw his tail from a heat stimulus. Statistical differences were not detected in tail flick analyses (Fig. 1) or nerve conduction studies between diabetic and control animals. This absence of neuropathy was unlike what we had previously reported in the less inbred Swiss Webster mouse, and again suggested that the C57BL/6J mouse was relatively resistant to complications when diabetes was induced by streptozotocin.

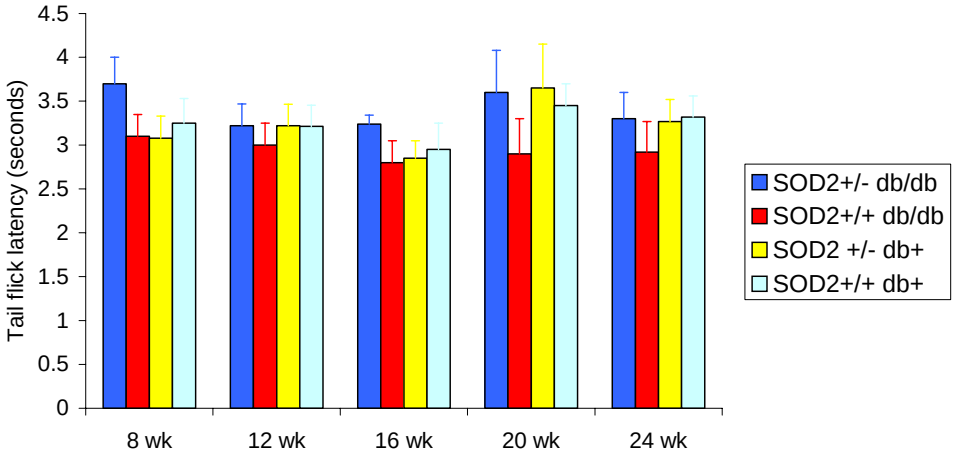

Fig. 1 Tail flick latencies measured in SOD2 c57Bl/6J mice

Year 2

SOD2 and db/db transgenic mouse models. In an attempt to identify another diabetic model with a higher likelihood of developing microvascular complications a genetic model of type 2 diabetes, the db/db C57BL/6J mouse, was bred to the SOD2 heterozygotes (+/-). The db/db mouse with a leptin receptor mutation is obese with insulin resistance and develops

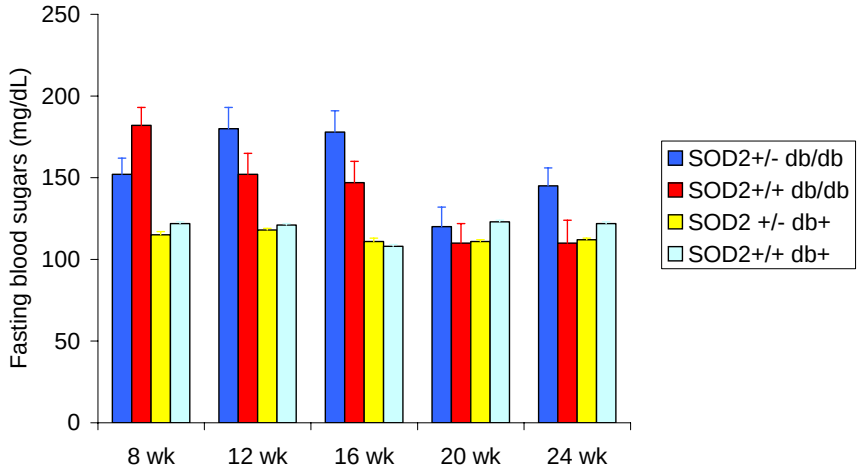

Fig. 2 Fasting blood sugars in C57BL/6J SOD2+/- and +/+ db/db and db+ mice

hyperglycemia by 4 weeks of age. An experiment with 10 animals per group was conducted over a 24 week period. The groups were: SOD2+/- db/db, SOD2+/+ db/db, SOD2+/- db/+ and SOD2+/+ db/+. The fasting blood sugar profiles of these mice are presented in Fig. 2. After 16 weeks, fasting tail blood glucoses in the db/db mice began to normalize and by 24 weeks, had attained essentially normoglycemic levels. The 28 week glycated hemoglobin data parallel the fasting blood glucose levels but remained mildly elevated at the end of the trial.

In the first 12 weeks of diabetes, db/db mice, regardless of their SOD2 genotype, had prolonged tail flick times of greater than 10 sec, highly significantly different from db/+ mice. By week 16, as fasting blood sugars approached more normal levels, the tail flicks of the db/db mice were less than 10 msec, but still significantly longer than db/+ animals. This downward trend appears to continue at weeks 20 and 24, although the number of animals with measurable sensory loss by tail flick was small (Fig. 3). Like the tail flick analyses, the nerve conduction studies (tail motor distal latency, tail sensory and sciatic nerve conduction velocities) remained

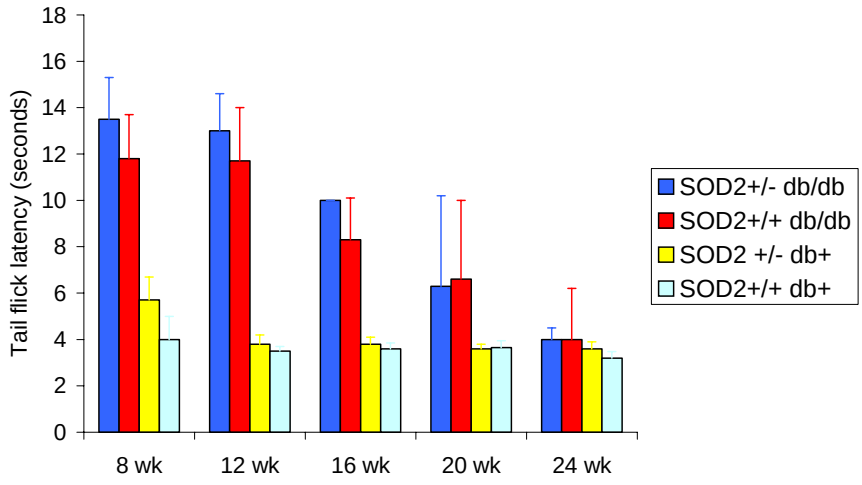

Fig. 3. Tail flick latencies in SOD2Db c57Bl/6J mice

abnormal but not to the degree we have previously observed in the mutant leptin receptor rat model, the Zucker rat, or to the initial degree of abnormality observed when hyperglycemia was high (e.g., at 12 weeks) (Fig. 4). Collectively these data show impaired neural function due presumably to a combination of hyperglycemia and insulin resistance in the db/db animal, with a suggestion of a modest decrease in overall impairment as the animal becomes more normoglycemic. There was no statistically significant additive effect of the SOD2 +/- genotype.

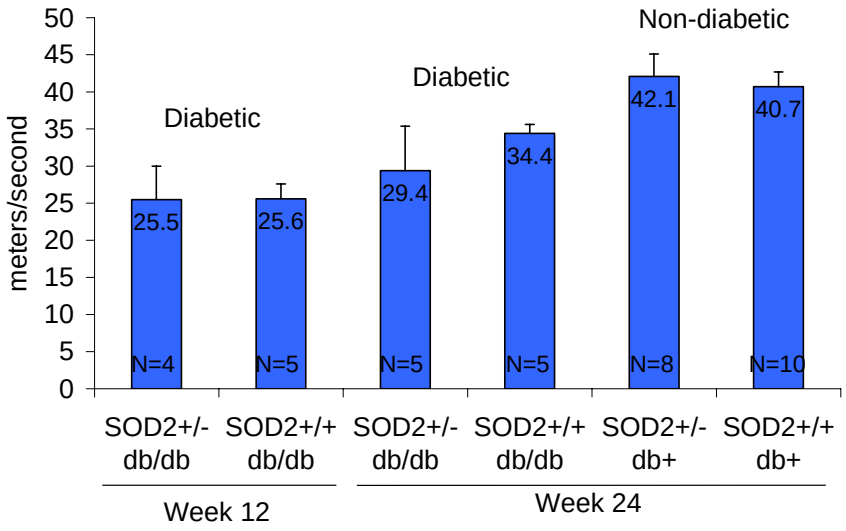

Fig. 4. Sciatic motor nerve conduction velocities at 12 and 24 weeks.

Targeted SOD2 mice and neuron specific SOD2 -/- mice. As we were preparing to initiate embryonic stem cell injections with our "floxed" SOD2 gene construct, we learned of the availability of a mouse line in which SOD2 had already been similarly targeted. In collaboration with AMDCC investigators at Vanderbilt University (Drs. Harris and Breyer) we obtained these mice to breed neuronal-specific Cre mice. These animals were received in the latter half of year 2. The colony was expanded and a breeding strategy was established to secure populations of neuronal-specific Cre//SOD2 loxP/loxP and SOD2 loxP/loxP littermates. These models are currently being studied in year 3 (see below).

Aldose reductase transgenic x SOD2 +/- mice. Although enhanced aldose reductase activity has been correlated to diabetic complications, especially neuropathy, diabetic aldose reductase overexpressing (AR tg) mice show only a mild increase in neuropathic findings when compared to control diabetic mice. Dr. Stevens, our collaborator, has found that the diabetic AR tg mice have a profound reduction in oxidative stress in the peripheral nerve when compared to diabetic control mice due to an increase in SOD activity. Therefore, in order to restore the full effect of aldose reductase activity on neuropathic changes, the AR tg mouse was crossed with the SOD2 +/- mice to generate AR tg//SOD2 +/- progeny. These mice are currently being studied in year 3 (see below).

<u>Beginning of Year 3</u>

Targeting the SOD2 gene and neuron-specific deletion. In order to perform neuron specific targeted deletion of the SOD2 gene, we cloned the murine SOD2 gene and created a

targeting vector encoding a portion of the murine SOD2 gene in which exons 1 and 2 were flanked by LoxP sites to allow for Cre recombinase directed excision of the area encompassed by the LoxP sites. During this time both the synpasin Cre and nestin Cre mice were validated for specific and effective expression of Cre recombinase. Synapsin Cre and nestin Cre mice were crossed with the Rosa26 mouse which expresses an interrupted "floxed" insert in the LacZ gene in all tissues. In the resultant progeny, Cre recombinase excises the "floxed" insert and thereby activates the LacZ gene. Cells in which Cre recombinase is expressed at sufficient levels to excise segments flanked by LoxP sites will be stained blue with X-gal in tissue sections. In the progeny of the Synapsin Cre x Rosa26, and nestin Cre x Rosa 26, neurons of both the central and peripheral nervous systems stained blue indicating sufficient expression of Cre recombinase.

Neuronal specific Cre mice. As described above, we crossed the synapsin and nestin Cre mice with the Rosa 26 mouse. We characterized the expression of β-galactosidase in the progeny of these crosses at postnatal days 1, 7, 14, 21 and in adult mice Three to 4 mice were examined per time point. In the nestin Cre x Rosa26 mice β-galactosidase was localized within neurons of the dorsal and ventral horn of the spinal cord, large and small sensory neurons of the dorsal root ganglia (DRG), and prevertebral sympathetic neurons. Not all neurons were positive for β-galactosidase activity; morphometric analysis to determine the percentage of DRG neurons in which the reporter gene is activated is ongoing. In the synapsin Cre x Rosa26 mice β-galactosidase was detected in the brain and DRG. Because nestin expression occurs in complications prone peripheral and autonomic neurons, we have bred the nestin-Cre mice with the floxed SOD2 mice and are waiting for sufficient numbers of mice to begin diabetes induction with streptozotocin.

GCLC+/- db/db mice. The γ-glutamate cysteine ligase (GCLC) heavy chain was targeted for disruption to produce a glutathione knockout mouse by two independent groups. This enzyme is an essential enzyme in glutathione synthesis. Homozygous disruption of the heavy subunit of GCLC is embryonically lethal. In contrast, the GCLC +/- mice are viable but show

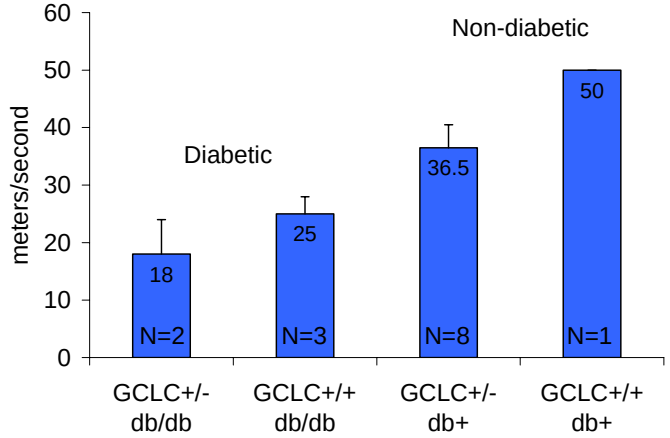

Fig. 5 Sciatic motor nerve conduction velocities at 16 weeks.

substantial decreases in GCLC protein and activity, and an approximately 20% decrease in glutathione levels. Thus, the GCLC +/- mouse should be a useful genetic model for mild endogenous oxidative stress, which could be substantially increased in diabetes. Given the resistance of normal C57Bl/6J mice to STZ diabetes, we bred these mice into the db/db C57BL/6J background resulting in 4 experimental groups: GCLC+/- db/db, GCLC+/+ db/db,

GCLC+/- db/+ and GCLC+/+ db/+. This trial is ongoing. By 16 weeks, there is a substantial decline in both tail flick and nerve conduction velocities (Fig. 5) in the db/db mice. While the numbers of mice tested are small, there is a suggestion that the GCLC+/- db/db animals are more prone to neuropathy than are the GCLC+/+ db/db mice. Again, this will be tested as more animals reach this timepoint.

Fig. 6. Effect of semisynthetic chow (AIN - 76A Diet) on blood glucose and weight in C57BL/6J db/db

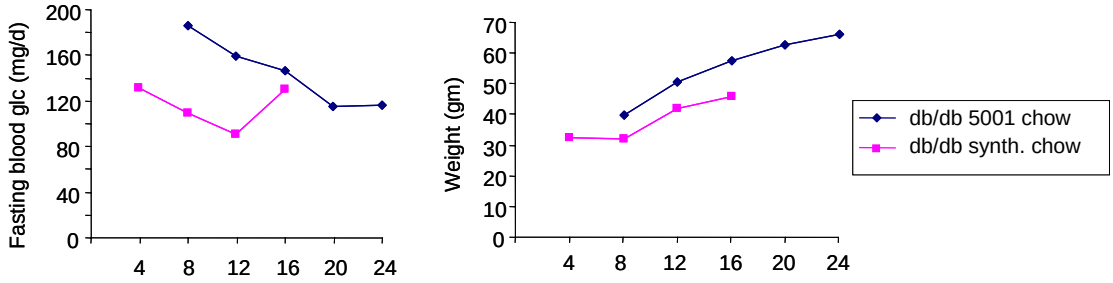

Effects of semisynthetic diet. The external advisory committee has expressed concern that lack of standardized, semisynthetic diets could result in skewed results due to variations in phytoestrogens or other hormones in regular rodent chow. Therefore, the GCLC db trial was performed with all animals on a semisynthetic diet (AIN - 76A Diet). The mice were given ad libidum access to the chow, but interestingly the db/db mice (whether GCLC +/+ or +/-) gained less weight than db/db mice on the regular Purina chow and developed fasting hyperglycemia that was even lower than levels in C57Bl/6J mice on a regular chow diet (Fig. 6).

Aldose reductase transgenic x SOD2 +/- STZ mice. These mice had NCV determinations 2 weeks after multiple low dose STZ injections. Motor nerve conduction velocities were reduced in the AR tg//SOD2 +/- mice (33 ± 4 m/sec) but not in the AR tg (46 ± 5 m/sec) or SOD2 +/- (41 ± 8 m/sec) animals. Many of the combined AR tg//SOD2 +/- animals died early from very severe hyperglycemia and were unavailable for nephropathy determinations. Although this model may be a difficult one to sustain over many months, we are hopeful that with small doses of insulin or even lower STZ administration, these mice will survive for 6 months of diabetes.

db/db C57BKS mice. AMDCC data over the past 2 years have now amply demonstrated that C57Bl/6J mice are relatively resistant to developing nephropathy and neuropathy. Although db/db C7BL/6J mice are more susceptible to microvascular complications than the STZ C57Bl/6J animals, this model remained generally resistant to progressive nephropathy and neuropathy despite genetic modifications. Moreover, as just noted, this model demonstrated a return to normoglycemia in several, though not all, of the AMDCC centers. In continued efforts to find the best genetically modified mouse for further neuropathy studies, we are completing the phenotyping of the KSLdb/db animals. Tail flick analysis (done at week 8) and sciatic nerve conduction studies (done at week 12) confirm significant neuropathy in these animals (Fig. 7), which will be further phenotyped when they reach 24 weeks.

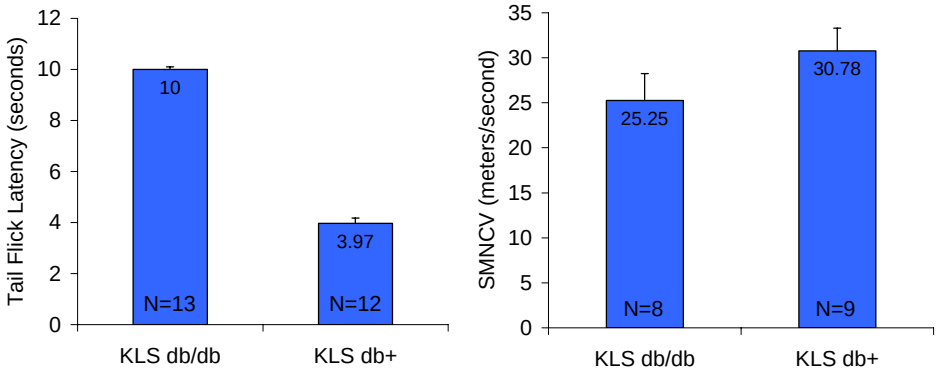

Fig. 7. Tail flick and sciatic motor nerve conduction velocities measured in KLS db mice.

Collaborations with other Groups:

Although many of our specific collaborations have been detailed in the progress report above, we have established the following intra-AMDCC collaborations:

1) Animals generated within the AMDCC group at the University of Michigan are phenotyped for the presence of neuropathy
2) Eyes (whole orb and retinas) will be sent to the Retinopathy Core at Cleveland Clinic
3) Bladder tissue will be sent to the Urology Core at Cleveland Clinic

Pertinent non-AMDCC Collaborations:

Listed below are the major collaborative projects related to the consortium goals but independent of AMDCC:

1) JDRF Center of Excellence for the study of diabetic complications. This center encompasses a number of collaborative projects exploring the role of glucose transporters, oxidative stress, SH2B-β, growth hormone receptors in diabetic complications. It also includes several clinical projects testing antioxidants and other agents in the treatment of diabetic complications. The Center Director is Dr. Feldman. Drs. Brosius, Russell and Stevens have projects in this center. Drs. Christin Carter-Su, and Ram Menon are non-AMDCC collaborators in this center.

2) Dr. Feldman is PI for several collaborative NIH grants investigating the etiology, pathogenesis and treatment of diabetic polyneuropathy. Dr. Russell is a co-investigators on several of these grants.

3) Dr. Feldman is an investigator in neuropathy aspects of the multi-institutional Epidemiology of Diabetes Interventions and Complications (EDIC) study.

4) Drs. Feldman and Brosius are PIs on grant proposals with Dr. Michael Uhler (University of Michigan) in a collaborative informatics project attempting to define a common set of transcriptional events that occur early in diabetic neurons and podocytes.

5) Dr. Stevens is the PI on several collaborative grants investigating myocardial aspects of diabetic autonomic neuropathy and is currently submitting an application with Dr. Feldman for proteomics research with regard to diabetes.

6) Dr. Russell is the PI on a NIH project investigating the role of IGF-I in oxidative stress and apoptosis in diabetic neuropathy; collaborators on this project include Drs. Feldman and Michael Brownlee (Albert Einstein College of Medicine). Dr. Russell is also the PI on a VA grant studying IGF-1 and Schwann Cells in neuropathy.

In summary, the major accomplishments in the first 2½ years of the AMDCC by the Neuropathy Phenotyping Core have been:

1) The development and validation of neuropathy phenotyping in mouse models and the neuropathy testing of several mouse models of diabetic neuropathy, including the establishement of tail flick and hind paw analgesia.
2) The development and testing of several mouse models of diabetic neuropathy.

C. Plans for the Coming Year

We will continue the phenotyping and development of mouse models of diabetic neuropathy. Our models are listed in Table 1 and discussed in Section B. Our goal is to phenotype models from other consortium members during year 3.

D. Significant Achievement

The most significant achievement of the Neuropathy Core is the development and validation of neuropathy phenotyping in mouse models.

E. Specific Methodology for Neuropathy Phenotyping

The techniques and protocols listed below relate the details of the neuropathy phenotyping procedures either in place or in development.

Evidence of clinical loss of sensory function

Tail Flick and Hind Paw Analgesia: In both humans and experimental animals, quantitative assessment of sensory function reflects the loss of nerve function. Heat thresholds are determined using a tail flick analgesia meter.

Mice are placed in an acrylic holder atop a tail flick analgesia meter (Stoelting, IL). The animal is placed in a restrainer so that its tail is in contact with an adjustable red light emitter adjusted in the range 60 – 170^{o} C. The animal flicks its tail out of the beam once its level of discomfort is reached. The time from activation of the beam to animal response is detected and recorded electronically. Plantar (hind paw) analgesia responses are obtained by placing the mice in a 6 chamber compartment using the same fiber optic heat source. The bottom of the compartment is maintained at 30^{o} C. The animals come to rest and the beam is maneuvered under the animal's hind paw. The operator then triggers the infrared beam. The rising temperature on the bottom of the foot causes the animal to move its foot. Latency is measured from activation of the beam to removal of the foot. These methods do not result in sensitization, and permit detection of potential different thermal-pain responses in the tail and foot. Both the left and right hind paws are measured with a space of at leas 5 min between measurements.

Electrophysiological evidence of nerve impairment
Nerve Conduction Studies (NCS): Methods to quantify nerve function include measures of impulse conduction. These methods have been adapted for use in rodents and are an accurate reflection of nerve health.

Before performing an electrophysiological examination, mice are anesthetized with ketamine 20-60 mg/kg and acepromazine 0.75 mg/kg by intraperitoneal injection. The hind limbs are kept injection free to avoid nerve or muscle injury. Nerve conduction studies are performed in the tail and left hind limb using platinum electrodes. Electrodes are placed adjacent to the nerve to obtain near nerve recordings. Tail nerve conduction is measured over a 4 cm distance from the base of the tail. Orthodromic tail compound muscle action potentials (CMAP) are obtained by recording at the tip of the tail and stimulating with the cathode 4 cm proximal to the G1 recording electrode. Orthodromic tail sensory nerve action potentials (SNAP) are obtained by stimulating at the tip of the tail and recording proximally. In the hind limb CMAP responses are recorded from the dorsal foot with stimulation proximally in the sciatic notch. Tail and limb temperature are maintained at least 32^{o} C.

Anatomical evidence of nerve fiber loss
Quantitation of Epidermal Nerve Fiber Density: Deficits in motor or sensory function may be caused by disruptions of axonal function or axonal loss. In order to characterize axonal loss caused by diabetes, skin biopsies are harvested following 24 weeks of neurophysiologic/sensory measures.

Mice are killed by an overdose of sodium pentobarbital and perfused with PLP (2% paraformaldehyde-lysine-periodate). Skin biopsies are harvested using dermal biopsy punches at the following sites; plantar surface of the right hind paw (foot pad), right leg, right thigh and right dorsal back. All areas (except for foot pad) will be gently shaved prior to dermal punch. The right side of the animal is preferred as the left side is used for nerve conduction studies. By sampling the sciatic nerve and skin from the right side of the animal, we are sure that the

anatomy has not been disrupted by needle puncture. Skin samples will be postfixed overnight in fresh PLP followed by cryoprotection in 5, 10 and 20% sucrose in phosphate buffer (PB, 0.1 M, pH 7.2). Skin samples will be embedded for cryo sectioning and oriented to collect sections that span from the epidermal surface to the deep dermis. 30 um serial sections will be collected onto Super Frost Plus slides and stored at -80 until stained. In order to assure accurate sampling, all sections will be collected and if any sections are lost it will be noted.

For immunohistochemistry (IHC), sections will be heated on a slide warmer (55^{o} C) for 10 minutes followed by; hydration in PB, 5 min; reduction of endogenous peroxidase activity, 0.05% H_2O_2 in PB, 10 min: 3, 10 min rinses in PB; and blocking and permeabilizing with 1% normal serum and 2% nonfat dry milk in PB containing 0.1% TX100. The sections are incubated in of primary antisera (rabbit anti-PGP 9.5, Chemicon) in a humid chamber at 22^{o} C for 16-24 hr. The following day, the sections are rinsed in PB; incubated with biotinylated goat anti-rabbit IgG; rinsed; incubated with avidin-horse radish peroxidase; and the chromogen developed with diaminobenzidine (DAB) in the presence of H_2O_2. The sections are not counterstained in order to optimize contrast between the DAB reaction product and the surrounding tissue.

Bright field images will be collected on a Nikon Microphot FXA upright microscope with a SPOT-RT digital camera. The DAB reaction product appears dark brown against an unstained background. These pixels will be converted to linear area by MetaMorph image analysis software.

Sections of skin not stained for PGP 9.5 may be stained for neurotransmitter markers. Other nervous system tissues are harvested and stored for future use. These include the brain and superior cervical ganglia. Sciatic nerves are harvested for biochemistry and potential examination by electron microscopy.

Advanced measures of neuropathy

As mouse phenotyping progresses and preferred animal models are identified, a detailed analysis of the neuroanatomy may be performed. These assays include; 1) transmission electron microscopy for evidence of oxidative stress induced mitochondrial swelling and cellular injury, including apoptosis, 2) poly TdT mediated dUTP-biotin nick end labeling (TUNEL) for evidence of DNA damage and 3) immunohistochemistry for cleaved caspase-3 and PARS (poly[ribose]).

Transmission Electron Microscopy (TEM): Mitochondria health may be measured by biochemical means (see below) and confocal microscopy using charge sensitive dyes. However, to assess the anatomical correlates of dysfunctional mitochondria, TEM is necessary to analyze ultrastructure. Small myelinated fibers, <5 μm in diameter and unmyelinated fibers are not accurately or reliably sampled at the light level. Therefore, TEM is used to analyze these populations of axons most affected by diabetes. Tissues to be used for TEM are postfixed in Trumps fixative (4% paraformaldehyde and 1% glutaraldehyde in 0.1 M phosphate buffer). Tissues are then embedded in Epon.

TEM for Mitochondrial Enlargement and Cellular Injury in DRG Neurons and Schwann Cells: TEM is still regarded as the "gold standard" for determination of cellular injury. Images are collected on a Phillips CM100 electron microscope using a Kodak MegaPlus digital camera. The TIF files are transferred and analyzed by MetaMorph. Mitochondrial enlargement, cellular injury and apoptosis are recorded for individual DRG neurons and SC. Mitochondrial and nuclear size are measured.

TEM for Axonal Morphology and Analysis of Small Myelinated and Unmyelinated Axons: Thin (90 nm) sections will be cut perpendicular to the plane of axon growth and photographs will be taken with the operator unaware of the treatment condition, using a Phillips CM100. Digital files collected from the Phillips CM-100 will be analyzed using MetaMorph (Universal Imaging Corp., West Chester, PA). This system allows for assessment of the total complement of sciatic nerve fibers and will provide the following measures: mean myelinated fiber size (μm^2), myelinated fiber density ($\#/mm^2$), coefficient of variation of fiber densities between image frames, myelinated fiber occupancy (percentage of endoneurial area occupied by myelinated fibers), and axon/myelin ratio. Briefly, the image will be "thresholded" to enhance contrast and select for objects of interest based on their defined gray levels. Further definitions of objects to be counted will include size and shape factors. The software will count these objects automatically and will be checked and corrected as necessary by a human reader. These measurements will be performed independently by two readers who will be unaware of the treatment the animal received.

TUNEL Staining: As cells undergo programmed cell death, the nuclear DNA is actively cleaved. These DNA “loose ends” are identified by application of a DNA repair enzyme tagged with digoxigenin. Therefore, TUNEL positive nuclei indicate the presence of active cellular and nuclear damage.

For staining of nuclei containing degraded DNA, tissue sections of DRG neurons and sciatic nerves (for SC) are labeled with digoxigenin-dUTP and then stained with horseradish peroxidase-conjugated anti-digoxigenin antibody (Intergen). The number of TUNEL positive neurons or SC are counted in each section and expressed as number of positive nuclei/µm2 fascicular area using MetaMorph digital capture available in the JDRF Morphometry core. Using digital imaging of the whole biopsy section, this software directs the motorized microscope stage to analyze each section of the nerve. Only clearly visible nuclei will be counted and serial sections will be separated by at least 20µm to avoid sampling the same nucleus twice.

Immunohistochemistry (IHC) for Markers of Programmed Cell Death: A number of enzymes and enzyme cleavage products mark the path to cell death. By localizing these proteins within neuronal and Schwann cell bodies, it is possible to determine if these cells are under attack from within.

Fixed neurons and SC or tissue sections are incubated with antibodies to cleaved (active) caspase-3 as well as whole (zymogen) caspase-3. By comparing the relative levels of cleaved to whole enzyme the number of cells actively undergoing cell death may be determined. PARs antibodies detect polyribosylated DNA, another marker of DNA damage. IHC for these

antibodies will be optimized but follows the basic protocol outlined above for PGP 9.5 staining. Both immunofluorescence and immunoperoxidase reactions are used depending on the need for dual labeling.

Biochemical Measures of Neuropathy: Oxidative stress is highly correlated with the metabolic changes caused by hyperglycemia. Increased levels of glucose overload mitochondria and result in the production of reactive oxygen species (ROS). In addition, the flow of excess glucose through cellular pathways decreases the cell's normal ability to detoxify ROS. As a result, the neurons and axons of the peripheral nervous system contain increased levels of ROS and decreased antioxidant capacity. The following assays are used to measure these changes in mouse models of diabetic neuropathy.

Measurements of Antioxidative Enzymatic Activities: For measurement of enzymatic activities ~20 mg of frozen sciatic nerves or DRG are homogenized in 2 ml of ice-cold 0.1 M sodium phosphate buffer, pH 6.5. Homogenates are centrifuged at 20,000 g and the supernatant fraction is used for assays of enzymatic activities and protein content. All measurements of enzymatic activities are performed at room temperature.

Superoxide Dismutase: Superoxide dismutase activity is measured according to Misra and Fridovich, by following spectrophotometrically (at 480 nm) the autooxidation of epinephrine at pH 7.4. The reaction mixture contains 0.8 ml 50 mM glycine buffer, pH 10.4 and 0.2 ml supernatant. The reaction is started by the addition of 0.02 ml (-)-epinephrine (due to poor solubility of (-)-epinephrine in water, the solution is prepared by suspending 40 mg of the compound in 2 ml water, and then by adding 2-3 drops of 2N HCI). SOD activity is expressed as nmol of (-)-epinephrine that are prevented from oxidation after addition of the sample compared to the corresponding readings in the blank cuvette. The molar extinction coefficient of 4.02mM-1cm-1 is used for calculations.

Catalase: Catalase activity is measured by following spectrophotometrically (at 240 nm) the decrease in absorbance of hydrogen peroxide after addition of the sample. The reaction mixture contains 0.9 ml 50 mM phosphate buffer, pH 6.8, containing 30% hydrogen peroxide(w/v), and the reaction is started by addition of the sample and is followed for 5 min. The enzyme activity is calculated using 2.04 mM-1cm-1 as molar extinction coefficient and is expressed in nmol hydrogen peroxide/mg protein per min.

Glutathione Transferase: Glutathione transferase activity towards 1-chloro-2, 4-dinitrobenzene (CDNB) is measured according to Habig et al. 0.8 ml of reaction mixture contains 0.1 M sodium phosphate buffer, pH 6.5, 1 mM GSH, 1mM CDNB dissolved in ethanol and 1 mM EDTA. The reaction is started by addition of 0.2 ml supernatant and is monitored spectro-photometrically at 340 nm for 5 min using an extinction coefficient of 9.6 mM-1cm-1.

Glutathione Reductase: Glutathione reductase activity is measured spectrophotometrically at 340 nm, by monitoring NADPH oxidation coupled to reduction of GSSG to GSH. 0.8 ml of reaction mixture contains 0.1 M potassium phosphate buffer, pH 7.0, 2.5 mM GSSG and 125 µM NADPH. The reaction is started by addition of 0.2 ml of the sample and is followed for 5 min. The calculations are performed by using a molar extinction coefficient of 6.22 mM-1cm-1.

Measurements of Antioxidants: Reduced glutathione (GSH) is assayed in perchloric acid extracts colorimetrically. Oxidized (GSSG) levels are determined spectrofluorometrically by an enzymatic procedure. The analytical mixture contains 0.8 ml 0.1 M imidazole buffer, 0.2 ml of the extract and 125 µM NADPH. The reaction is started by the addition of glutathione reductase.

References

1. Greene, D. A., Feldman, E. L., Stevens, M. J., Sima, A. A. F., Albers, J. W., and Pfeifer, M. A. Diabetic Neuropathy. *In:* Jr. D. Porte and R. Sherwin (eds.), Diabetes Mellitus, 5 ed, pp. 1009-1076. East Norwalk, CT: Appleton & Lange, 1997.
2. Wright, A. and Nukada, H. Sciatic nerve morphology and morphometry in mature rats with streptozocin-induced diabetes. Acta Neuropathol., *88*: 571-578, 1994.
3. Feldman, E. L., Stevens, M. J., and Russell, J. W. Diabetic peripheral and autonomic neuropathy. *In:* M. A. Sperling (ed.), Contemporary Endocrinology Humana Press, 2002.
4. Dyck, P. J., Karnes, J. L., and Daube, J. Clinical and neuropathological criteria for the diagnosis and staging of diabetic polyneuropathy. Brain, *108*: 861-880, 1985.
5. Dyck, P. J., Dyck, P. J. B., and Grant, I. A. Peripheral neuropathy - Reply. Neurology, *48*: 1140, 1997.
6. Feldman, E. L., Stevens, M. J., Russell, J. W., and Greene, D. A. Diabetic neuropathy. *In:* S. Taylor (ed.), Current Review of Diabetes, pp. 71-83. Current Medicine, 1999.
7. Windebank, A. J. and Feldman, E. L. Diabetes and the nervous system. *In:* M. J. Aminoff (ed.), Neurology and General Medicine, 3rd ed, pp. 341-364. Churchill Livingstone, 2001.
8. Feldman, E. L., Stevens, M. J., Russell, J. W., and Greene, D. A. Diabetic neuropathy. *In:* K. L. Becker (ed.), Principles and Practice of Endocrinology and Metabolism, 3rd ed, pp. 1391-1399. Philadelphia: Lippincott Williams & Wilkins, 2001.
9. Feldman, E. L., Stevens, M. J., Russell, J. W., and Greene, D. A. Somatosensory neuropathy. *In:* D. Porte, Jr., R. S. Sherwin, and A. Baron (eds.), Ellenberg and Rifkin's Diabetes Mellitus, 6th ed, pp. 771-788. McGraw Hill, 2002.
10. Stevens, M. J., Obrosova, I., Pop-Busui, R., Greene, D. A., and Feldman, E. L. Pathogenesis of diabetic neuropathy. *In:* D. Porte, Jr., R. S. Sherwin, and A. Baron (eds.), Ellenberg and Rifkin's Diabetes Mellitus, 6th ed, pp. 747-770. McGraw Hill, 2002.
11. Greene, D. A., Obrosova, I., Stevens, M. J., and Feldman, E. L. Pathways of glucose-mediated oxidative stress in diabetic neuropathy. *In:* L. Packer, P. Rosen, H. J. Tritschler, G. L. King, and A. Azzi (eds.), Antioxidants in diabetes management, pp. 111-119. New York: Marcel Dekker, 2000.
12. Feldman, E. L. Oxidative stress and diabetic neuropathy: a new understanding of an old problem. J Clin. Invest, *111*: 431-433, 2003.